A Public dynamic PET brain database for lesion detection and quantification

First Authors: Natalia Martinez, Martin Bertran.
Co-authors: Guillermo Carbajal, Alicia Fernandez and Alvaro Gomez.

Abstract— **Purpose: Dynamic PET imaging gives insight into various metabolic processes. Considerable work has been carried out with the aim of facilitate visual inspection and interpretation of the studies. However, comparison between different algorithms and methods is an arduous task. Source codes are rarely distributed, and if available, there is no single, unified public database to test them on. Therefore, turns out mandatory for any new research team, to invest considerable time and effort in acquiring or creating their own database before diving headlong into research. This paper presents a dynamic PET brain database.**
Methods: The ASIM and STIR software packages are used to simulate and reconstruct phantoms based on a pharmacokinetic model activity.
Results: There are 18 phantoms in total, each with 5 implanted regions, and with varying lesion activities.
Conclusions: Phantoms are made available to the community. We hope this makes intercomparisons between algorithms easier, as well as accelerate the research process in the area.

I. INTRODUCTION

Functional imaging is a method in medical imaging of detecting or measuring changes in metabolism, blood flow, regional chemical composition, and absorption. Positron Emission Tomography (PET) is one amongst these techniques, it can produce 3D and 4D (dynamic) images, and its most common use is for the exploration of cancer metastasis using the FDG tracer.

The recent use of dynamic PET scans enables a new range of analysis techniques, but the lack of a public phantom database makes comparing tests between researchers a difficult task, and requires that research groups spend time and effort making their own database before starting their research work.

This is exemplified in [12], [13], where researchers must not only present their work, but create and describe their private database, this consumes valuable research time, as well as making intercomparisons more tedious.

In this article, we present a public dynamic PET brain phantom database for the FDG tracer. Additionally the methodology used to generate these phantoms using the ASIM [3], [8] simulator and the STIR [4] reconstruction software is presented.

II. MATERIALS AND METHODS.

In order to simulate a realistic phantom, it is necessary to define four main items.

- Anatomy: The volume of interest, as well as the different regions are defined. In this case, the volume attempts to emulate the contents of a human head.
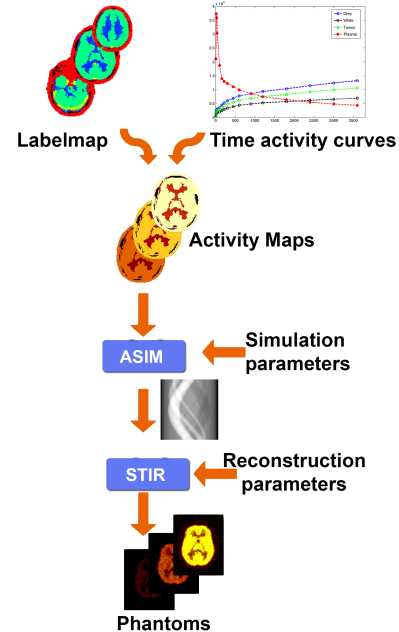

Fig. 1: From top to bottom: The labelmap is combined with the defined activity curves to generate the activity maps. These are used as input for the ASIM simulator, which outputs the raw acquisitions (sinograms). These sinograms are reconstructed using the STIR software to obtain the final 4D phantom.

- Activity: Defines how each region's activity changes over time. To generate this activity, the two compartment pharmacokinetical model is used.
- Acquisition: Controls how a given anatomy with a given activity is acquired or observed by a dynamic PET scan. To perform the simulated acquisition, we use the ASIM simulator [3], [8].
- Reconstruction: This process turns the acquired data (sinograms) into an easy to interpret 3D (or 4D) image. Reconstruction is performed using the STIR library [4].

In Figure 1, the workflow used to generate a dynamic PET phantom is outlined.

We now give additional details on the implementation of each of the aforementioned steps.

A. Anatomy: Labelmaps

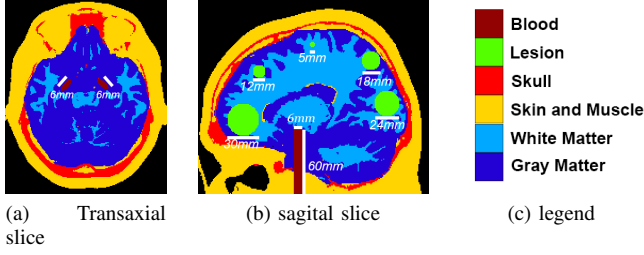A three-dimensional (3D) software phantom was created based on the BrainWeb database [2]. Two $6cm$ long and

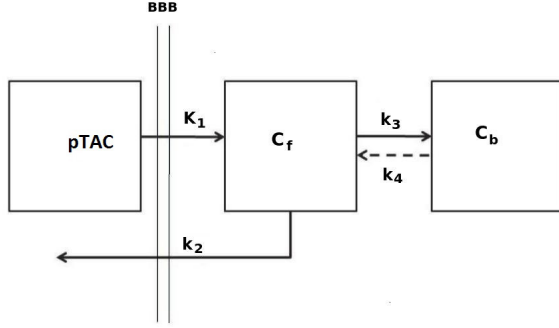Fig. 2: Transaxial and sagital slices of the defined labelmap.

Fig. 3: Two compartment model: Tracer enters the free compartment from arterial plasma through the Blood Brain Barrier (BBB) at a rate K_1, and leaves back into bloodstream at a rate k_2. The tracer is metabolized from the free compartment at a rate k_3

$6mm$ across carotid arteries were implanted on top of the prelabeled normal brain anatomical model available at this database.

For all phantoms, additional spherical regions were added with diameters ranging from $30mm$ to $4mm$.

The labelmap was then simplified into seven regions: [Background, Grey Matter, White Matter, Carotid arteries, Lesion, Skin, Skull].

The final labelmap can be seen in Figure 2

B. Compartment model

The pharmacokinetics on FDG are usually described by the 2-tissue compartment model seen in figure 3. The model input function, denoted as $pTAC$ describes the tracer concentration in arterial blood plasma. The concentration curves C_f and C_b represent the free and bound tracer concentration in tissue respectively.

The rate constants used in the model are the uptake rate from blood to free tracer in tissue, $K_1[\frac{ml}{g \times min}]$, the tissue clearance rate, $k_2[\frac{1}{min}]$ and the rates of exchange between free and trapped tracers in tissue $k_3[\frac{1}{min}]$ and $k_4[\frac{1}{min}]$. The parameter $V_a[\frac{ml}{g}]$ represent the fraction of arterial blood in the tissue.

The observed tissue concentration (C_{tissue}) contains the sum of C_f and C_b. The system under study can be described

TABLE I: pTAC model constants

Constants	Values
$A_1[MBq]$	31.5
$A_2[kBq]$	770
$A_3[kBq]$	809
$\lambda_1[1/min]$	−4.13
$\lambda_3[1/min]$	−0.0104
$\lambda_3[1/min]$	−0.1191

with the following matrix representation:

$$\begin{bmatrix} \frac{dC_f}{dt} \\ \frac{dC_b}{dt} \end{bmatrix} = \begin{bmatrix} -(k_2 + k_3) & k_4 \\ k_3 & -k_4 \end{bmatrix} \times \begin{bmatrix} C_f \\ C_b \end{bmatrix} + \begin{bmatrix} K_1 \\ 0 \end{bmatrix} \times pTAC \tag{1}$$

$$C_{tissue} = \begin{bmatrix} 1 & 1 \end{bmatrix} \times \begin{bmatrix} C_f \\ C_b \end{bmatrix} + \begin{bmatrix} 0 \end{bmatrix} \times pTAC \tag{2}$$

Analytically, C_{tissue} can be written as a function of the input function $pTAC$ as follows:

$$C_{tissue}(t) = \frac{K_1}{\alpha_2 - \alpha_1} pTAC(t) \otimes$$
$$\otimes [(k3 + k4 - \alpha_1)e^{-\alpha_1 t} + (\alpha_2 - k_3 - k_4)e^{-\alpha_2 t}]$$

Where $\otimes$ denotes the temporal convolution and

$$\alpha_{1,2} = \frac{k_2 + k_3 + k_4}{2} \pm \frac{\sqrt{(k_2 + k_3 + k_4)^2 - 4k_2 k_4}}{2}$$

A very useful parameter to measure is the metabolic flux constant, denoted as $K_I[\frac{ml}{g \times min}]$, it is defined as: $K_I = \frac{K_1 k_3}{k_2 + k_3}$ and represents the average rate of influx from arterial plasma into tissue.

In a PET image, each voxel or volume of interest (VOI) is the mix of the activity on the blood vessels within the region and the tissue activity. This can be represented as follows: $C_{PET} = (1 - V_a)C_{tissue} + V_a pTAC$ Where V_a is the proportion of blood to voxel.

C. Definition of activity curves

There are three defined tissue regions (White matter, Grey matter, and lesion or tumor), each with its own associated activity curve.

As mentioned previously, for a given region i, its associated activity curve can be expressed as:

$$tTAC_i = (1 - V_{a_i})C_{tissue_i} + V_{a_i} pTAC.$$

The input function $pTAC$ is created using the proposal outlined in [1], and has the following expression:

$$pTAC(t) = A_1(t - A_2 + A_3)e^{\lambda_1 t} + A_2 e^{\lambda_2 t} + A_3 e^{\lambda_3 t}$$

The constants used to create the $pTAC$ activity curve are shown in Table I, and were extracted from [1].

The tissue activities are then calculated using the Matlab control system toolbox package [14]. Tissue activities are calculated for a period of one hour, with samples calculated for each second.

TABLE II: Compartmental model constants

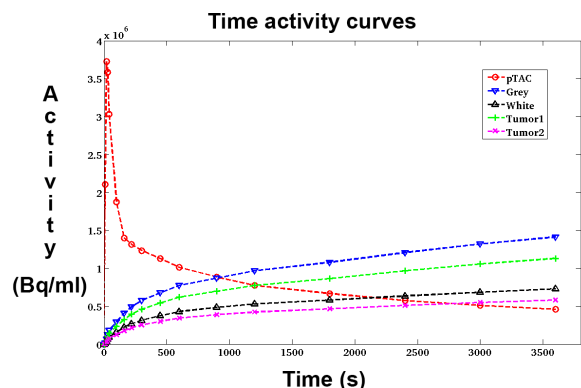| Tissue	K_1	k_2	k_3	k_4	V_a
Gray matter	0.102	0.13	0.062	0.0068	0.058
White matter	0.054	0.109	0.045	0.0058	0.025

Fig. 4: Activity curves generated for the simulated phantoms. $Tumor_1$ has 20% less activity than normal grey tissue, while $Tumor_2$ has 20% less activity than normal white tissue.

Table II shows the kinetic constants (k_i) s used to generate the tissue activities, based on the constants used in [6].

For tumors, lesion activity was taken to be a fraction of the normal white and grey matter activity, three fractions were evaluated: $[70\%, 80\%, 90\%]$.

Using these constants, and the defined pTAC, activity curves result as shown in Figure 4.

D. Definition of activity images

The activity curves must be combined with the labelmap to define an activity image volume for each frame. Each region is assigned the mean activity value of its tissue type for the duration of the frame.

The utilized frame definition is the standard 16 frames with variable time lengths:

$$4 \times 10s, 4 \times 60s, 2 \times 150s, 2 \times 300s, 4 \times 600$$

Once a frame definition has been chosen we proceed to sample the activity curves (pTAC and tTACs).

Given a frame T_F with a duration of ΔT_F starting at T_{Fi} and ending at time T_{Ff} we sample the activity curve as:

$$TAC(T_F) = \int_{T_{Fi}}^{T_{Ff}} \frac{TAC(t)}{\Delta T_F} dt$$

Finally we generate one activity image for each frame using the sampled TACs.

E. Simulation parameters

The ASIM simulator consists of three core modules:

- Simul: Generates noiseless PET emission and attenuation sinograms. It is also possible to set the PSF of the emulated scanner.

TABLE III: Simulated phantom lesion activity and noise

Lesion /α noise	5×10^{-6}	5×10^{-5}	5×10^{-4}
70% GM	$70GMa6$	$70GMa5$	$70GMa4$
80% GM	$80GMa6$	$80GMa5$	$80GMa4$
90% GM	$90GMa6$	$90GMa5$	$90GMa4$
70% WM	$70WMa6$	$70WMa5$	$70WMa4$
80% WM	$80WMa6$	$80WMa5$	$80WMa4$
90% WM	$90WMa6$	$90WMa5$	$90WMa4$

- Noise: Applies Poisson distributed noise to a sinogram. Noise is based on the number of true, random, and scatter photon counts.
- Normalize: Applies corrections to these datasets.

The phantoms were simulated with an isotropic Gaussian PSF function with $FWHM = 6mm$. In order to apply the noise, we only used true counts, without simulating scattered or random photons.

In our work we used the following formula to calculate the true counts for each frame T_F:

$$n(T_F) = \alpha \times \Delta T_F \times \bar{C}_{PET}(T_F) \times e^{\frac{-T_F}{\tau}}$$

Where $n(T_F)$ are the true counts for frame T_F, $\Delta T_F \times \bar{C}_{PET}(T_F)$ represents the number of photons emitted by the sample before taking the decay factor into account, $e^{\frac{T_F}{\tau}}$ is the exponential decay factor for frame T_F, α is a calibration factor used to vary the overall noise level of the entire simulation. The utilized alpha values are as follows:

$$\alpha = [5 \times 10^{-6}, 5 \times 10^{-5}, 5 \times 10^{-4}]$$

F. Reconstruction

The sinograms thus obtained from the simulation are reconstructed using the STIR software package using the FBP2D algorithm. The simulation and reconstruction parameters are chosen based on the ECAT HR+ PET scanner specifications, using the default .par files provided by ASIM.

III. RESULTS

Phantoms were simulated at three distinct noise levels and with varying lesion activity.

There are 18 phantoms in total, 6 different lesion activities ($70\%, 80\%$ and 90% of regular white and grey matter activity), acquired at 3 different noise levels ($\alpha = [5 \times 10^{-6}, 5 \times 10^{-5}, 5 \times 10^{-4}]$). This is summarized in Table III

In the presented database, we provide:

- labelmap.
- Ground truth of activity curves.
- Emission and noise sinograms.
- FBP2D reconstructed phantoms.

As a usage example, we present the analysis of the phantoms using the 3D Slicer open software for medical imaging visualizaton [9], [10], utilizing the dPETBrainQuantification extension module [11]. With it, the vasculatures present in the scan are detected (see Figure 5), the pTAC signal is extracted from these vasculatures, and a Patlak [5] graphical analysis is done on a pixel by pixel basis.
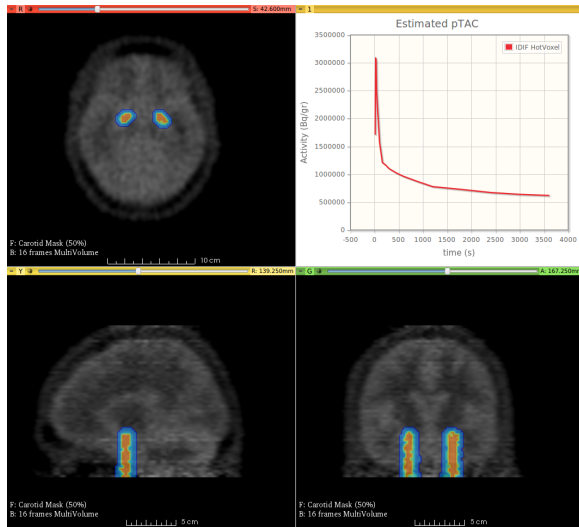
Fig. 5: Segmented carotids and adjacent tissue are highlighted in the transversal, coronal and sagital slices. The displayed graph is the estimated pTAC using dPETBrain-Quantification HotVoxel method.

(a) sagital slice, lesion free

(b) lesions hightligthed in the sagital slice

(c) lesion shown in coronal slice ($24mm$)

(d) lesion shown in coronal slice ($30mm$)

(e) lesion shown in coronal slice ($18mm$)

Fig. 6: Implanted lesions shown in Patlak Map. Lesions consume 80% of normal white and grey matter.

Visually, the most easily located lesions in the Patlak map are the three largest ones ($30mm$, $24mm$ and $18mm$). In figure 6 the Patlak map of one of the phantoms is shown, and the detected lesions are highlighted.

IV. CONCLUSIONS AND FUTURE WORK

In this paper we proposed a public database. This database is relatively easy to use and interpret. It is also easily expandable to different labelmaps, tracers, frame definition and reconstruction algorithms. Even though the phantoms are not anatomically complex, the database can be used for segmentation, detection, quantification and performance evaluation

The simulation and reconstruction software used are popular and well documented. Simulation times are manageable, particularly when using parallel processing for simulating multiple frames simultaneously, which allows for fast and easy prototyping.

The database is made available at [1]

It is the author's hope that this database receives user feedback, in order to better accomplish the work of intercomparable and peer reviewed PET processing methods.

ACKNOWLEDGEMENT

REFERENCES

[1] Feng, D., Wang, X., & Yan, H. (1994). A computer simulation study on the input function sampling schedules in tracer kinetic modeling with positron emission tomography (PET). Computer methods and programs in biomedicine, 45(3), 175-186.
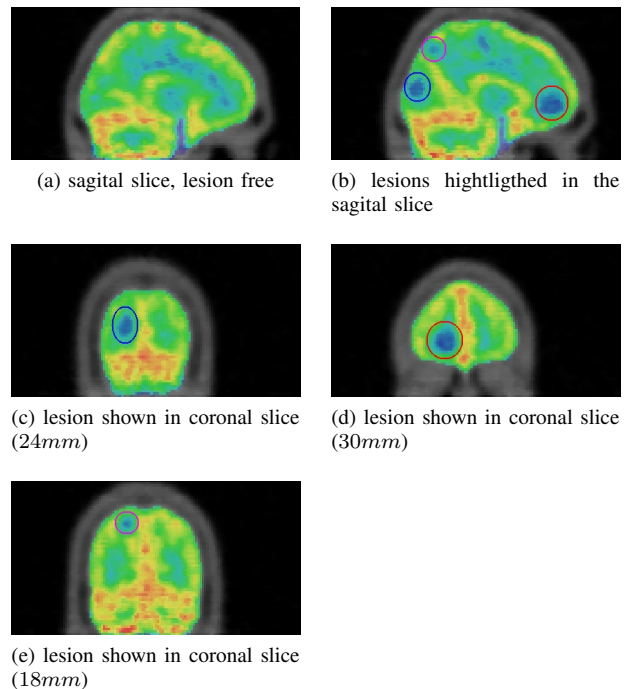
[2] (2015) BrainWeb. [Online]. Available: www.bic.mni.mcgill.ca/brainweb/

[3] (2015) ASIM [ONLINE] Analytic PET simulator Home Page (Online). University of Washington.,Fr om:http://depts.washington.edu/asimuw/

[4] Thielemans, K., Tsoumpas, C., Mustafovic, S., Beisel, T., Aguiar, P., Dikaios, N., & Jacobson, M. W. (2012). STIR: software for tomographic image reconstruction release 2. Physics in medicine and biology, 57(4), 867.

[5] Patlak CS, Blasberg RG. Graphical evaluation of blood-to-brain transfer constants from multiple-time uptake data. Generalizations. J Cereb Blood Flow Metab. 1985; 5: 584-590.

[6] Phelps ME, Huang SC, Hoffman EJ , Selin C, Sokoloff L , Kuhl DE (1979) Tomographic measurements of local cerebral glucose metabolic rate in humans with [F18]2-fluoro-2-deoxy-Dglucose: validation of method. Ann Nellrol 6 : 3 7 1 - 388

[7] (2015) Matlab [ONLINE] http://www.mathworks.com/help/matlab/

[8] Elston, B. (September 24 2009). Introduction to ASIM 2.1.1: A PET Analytic Simulator. Proceedings from Imaging Research Laboratory Scientific Retreat Conference Record, Seattle, WA

[9] A. Fedorov et al. , ?3D slicer as an image computing platform for the quantitative imaging network,? Magn. Reson. Imaging , vol. 30, pp. 1323?1341, 2012.

[10] (2015) Slicer [ONLINE] http://www.slicer.org/

[11] (2015) dPETBrainQuantification wiki [ONLINE] http://wiki.slicer.org/slicerWiki/index.php/Documentation/4.4/Modules/dPetBrainQuantification

[12] Baete, K., Nuyts, J., Van Paesschen, W., Suetens, P., & Dupont, P. (2003, October). Evaluation of an anatomical based MAP reconstruction algorithm for PET in epilepsy. In Nuclear Science Symposium Conference Record, 2003 IEEE (Vol. 3, pp. 2017-2021). IEEE.

[13] Hagstrom, I., Schmidtlein, C. R., Karlsson, M., & Larsson, A. (2014). Compartment modeling of dynamic brain PET The impact of scatter corrections on parameter errors. Medical physics, 41(11), 111907.

[14] (2015) Matlab [ONLINE] http://www.mathworks.com/products/matlab/

[1] http://iie.fing.edu.uy/~agomez/phantomweb